An Inverse Method of Designing the Cooling Passages of Turbine Blades Based on the Heat Adjoint Equation

DOI: 10.1177/0957650913518911

available online: http://pia.sagepub.com/content/228/3/328.

An inverse method of designing the cooling passages of turbine blades based on the heat adjoint equation

Michele Ferlauto
Department of Aerospace and Mechanical Engineering, Politecnico di Torino
Corso Duca degli Abruzzi 24, 10129 Turin, Italy.
E-mail *: michele.ferlauto@polito.it*

Abstract

A method of solution of the inverse problem in heat conduction is presented. The method, based on an adjoint optimization procedure, is applied to the design of the pattern of cooling passages inside turbine blades. For blade coating technologies, the general case of a non-homogeneous solid material is considered. The numerical solution of both the temperature field and of the adjoint problem is based on a finite element method. The new formulation of the adjoint thermal problem is deduced for three different parametric representation of the internal cooling passages. This allows the designer to select the most adequate blade parametrization, going from blades with circular coolant passages to modern multi-holed hollow blades. The mathematical method, the adjoint problem solution and the enforcement of geometric constraints are explained and the procedure is validated against theoretical, experimental data and numerical solution available in open literature.

Keywords. Inverse problem, heat conduction, adjoint methods.

[1]

1 INTRODUCTION

A wide range of engineering problems in thermal analysis and design have been formulated as inverse heat transfer problems [1, 2, 3, 4]. The inverse problem involves the estimation of the cause by utilizing the knowledge of the effect. Several studies focus on the cause-effect relationship between heat flux and temperature. A classical example deals with the estimation of an unknown boundary heat flux, by using temperature measurements taken below the boundary surface. The design problem itself can be formulated as an inverse problem in which some conditions are given at the boundary, while the shape of the body contour that realizes the imposed thermal features is unknown. Applications of this approach to heat conduction design problems have been proposed and successfully applied to turbine blade cooling in the last three decades. By using inverse methods, the thermal design of turbine blades has been solved for circular [5], super-elliptic [6], and generic geometries of the internal cooling passages [7, 8]. The numerical procedures are mainly based on a direct solver driven by an optimization method. In one of the earliest applications [5] a Boundary Element Method (BEM) for heat conduction analysis and a gradient method, the Steepest Descent Method (SDM), was used to converge to the inverse problem solution. Since then, the exponential growth of computational resources has allowed for an extensive use of more flexible and CPU consuming numerical approaches. Solvers based on the Finite Element Method (FEM) or Finite Volume Method (FVM) in two and three dimensions have been used to evaluate the thermal field, while, in the modelling of the physics of heat transfer, the convection and radiation effects have been included. Subsequently the research has evolved to conjugate heat transfer analyses by including the mutual interactions with the fluid flow and by modelling film cooling effects [9].

In the field of optimization, the improvements of gradient based methods have lead to the various formulations by adjoint methods for 2D/3D problems [8, 10, 11], while the use of Genetic Algorithms (GA) has been also introduced for the solution of the single objective and multi-objective optimization problems. A new impulse to thermal design in aerospace propulsion comes from recent efforts to design aeroengines which meet the Vision 2020 requirements on gasturbine emissions and efficiency from Advisory Council for Aeronautics Research in Europe (ACARE). A direct way to enhance efficiency is obtained by increasing the maximum cycle temperature, i.e. the temperature into the combustion chamber. Moreover, other investigations introduce the Interstage Turbine Burner (ITB) concept to modify the thermodynamic cycle during flight, going towards variable cycle aeroengines. In both approaches a closer control of the temperatures is required and the thermal design of some of the engine components, such as the burners and the turbine blades, becomes more aggressive. In this scenario, automated inverse problem solvers can help the designer to make choices based on a wider investigation of the design space.

In the present work an approach to the inverse problem solution is proposed. The method is based on adjoint optimization and follows the footsteps of a technique of aerodynamic design [12, 13]. The mathematical treatment of the adjoint problem differs from previous adjoint approaches (e.g. see [8, 11]). In fact, the proposed formula-

[1] Please send correspondence to:
Michele Ferlauto
Dept. of Mechanical and Aerospace Engineering, Politecnico di Torino,
c.so Duca degli Abruzzi, 24 - 10129 Torino, Italy
phone: +39 011 0906834 telefax: +39 011 0906899
e-mail*: michele.ferlauto@polito.it*

tion does not need a sensitivity problem to be solved and it includes a penalization for imposing geometrical constraints. To allow for the treatment of coated blading, the heat conduction equation in a non-homogeneous material has been considered. A FEM approach has been used both to compute the thermal field inside the turbine blade and to solve the adjoint problem. The case of circular cooling passages has been treated in [14] in detail, covering the related mathematical and numerical aspects. In the present work, the design method is extended to the complex geometry of modern turbine blades by introducing suitable parametrizations for cooling flow passages of a general shape and which also have some portions of the contour already fixed by other geometrical constrains.

The paper is organized as follows: in the next section the mathematical model and the inverse problem solution are presented. Then the adjoint problem is derived and the numerical technique is explained. The geometric parametrizations of the blade cooling passages are discussed and the mathematical implications in both the inverse problem and the adjoint optimization are derived. Finally the procedure is validated against an analytical solution and against test-cases based on experimental data available in the open literature.

2 MATHEMATICAL MODEL

We consider the heat conduction equation in a non-homogeneous material and Robin boundary conditions. This set of equations may be written in compact form as:

$$\nabla \cdot (k \nabla T) = 0 \qquad on\ \Omega \tag{1a}$$

$$k \frac{\partial T}{\partial n} = h(T_g - T) \qquad on\ \Gamma = \Gamma_b \tag{1b}$$

$$k \frac{\partial T}{\partial n} = h(T - T_{cj}) \qquad on\ \Gamma_c = \bigcup_{j=1}^{M} \Gamma_j \tag{1c}$$

where T is temperature, $T_g,\ T_{cj}$ are gas and coolant flows temperatures, h is the local heat transfer coefficient, k the thermal conductivity and $\boldsymbol{n}$ is outward normal vector. We pose the thermal conductivity $k = k(\boldsymbol{x})$ as a function of the position vector $\boldsymbol{x}$. In fact, in turbine blades with ceramic coating one can distinguish two, or more, regions with very different $k-$values. A sketch of the domain representation is given in Figs 1-3. In all cases, Γ_b is the external surface of the turbine blade, Γ_a is the interfacial surface between inner core blade (light grey) and coating material (dark grey), and Γ_c is the union of the Γ_j surfaces of the M inner cooling passages. We assume that $h = h[\Gamma(s)]$ is a given function of the heat transfer process along the generic contour $\Gamma_j(s)$ and on the blade surface $\Gamma_b(s)$. The actual functional can be either the result of an experimental investigation (e.g. expressed is terms of the Nusselt number), either a polynomial fitting of an aero-thermal simulation. In the framework of the "core" of inverse technique, h is also supposed to include the 2D effects of various technologies for heat transfer enhancement (ribs, turbulators, pin fins).

In the classical thermal inverse problem the boundary

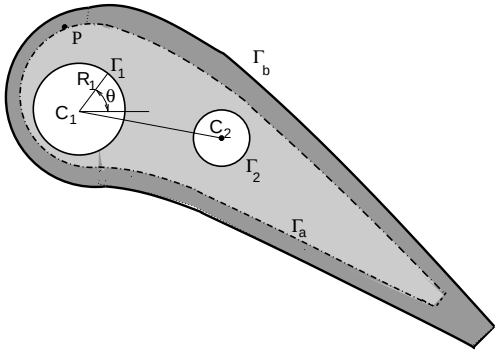

Figure 1: Domain geometry nomenclature for a blade with circular coolant passages (Parametrization A).

shape of the cooling passages Γ_j is regarded as unknown while some field variables are known at the external boundary Γ_b. In the literature, whatever the method of solution used, various choices has been adopted in formulating the the inverse problem. In [7] both the heat flux and the temperature are imposed in a discrete set of points on Γ_b. In [5] the temperature on Γ_b is imposed and the geometry that realizes a target heat flux distribution in Γ_b is sought for. In [8] mixed boundary conditions are imposed in both Γ_b and on Γ_j , while looking for the geometry of the cooling passages that realizes the desired temperature in a discrete set on points on Γ_b. In the present work the approach is similar to the latter case, which is, in our opinion, the most suitable for a direct application, as well as for the experimental validation. We impose Robin boundary conditions both on the external blade surface Γ_b and on the internal cooling passages Γ_j and we use an adjoint-based gradient method to find the hole locations and shape which realize a desired temperature distribution $T_b(\boldsymbol{x})$ along the boundary Γ_b. The temperature distribution $T_b(\boldsymbol{x})$ is here a given function, the result of a designer choice.

The numerical solution of system (1) is based on the Finite Element Method. The derivation of the solution for the steady conduction equation is a standard exercise in classical textbooks on FEM. The formulation implemented here can be found in [14]. The inverse problem is solved as an optimization problem, as outlined in the next section. The procedure iterates on a series of direct computations until all boundary condition and constraints are satisfied within an expected range of gradient and cost function residuals.

3 ADJOINT EQUATION AND GRADIENT

We define the cost function

$$\mathcal{F}(\Gamma_c, T) = \frac{1}{2} \int_{\Gamma_b} \left[T(\boldsymbol{x}) - T_b(\boldsymbol{x}) \right]^2 d\Gamma + \chi \mathcal{P}(\Gamma_c) \tag{2}$$

where the $\mathcal{P}(\Gamma_c)$ is a penalization function added to enforce the geometric constraints to the optimization problem. The control variable is the set of relations defining the cooling passages geometry Γ_c. All the parametrizations proposed for the coolant passage boundary could be

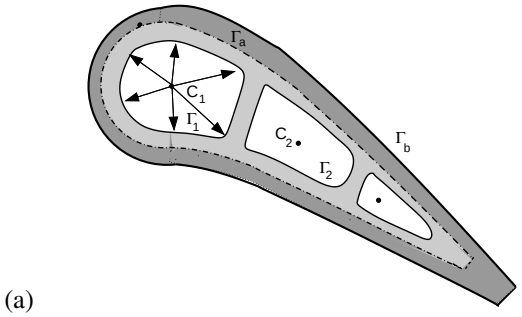

(a)

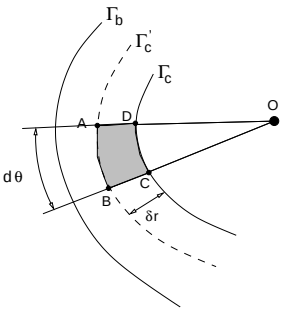

(b)

Figure 2: Domain geometry nomenclature (a) and domain area variation (b) for a blade with a centroids based representation of coolant passages (Parametrization B).

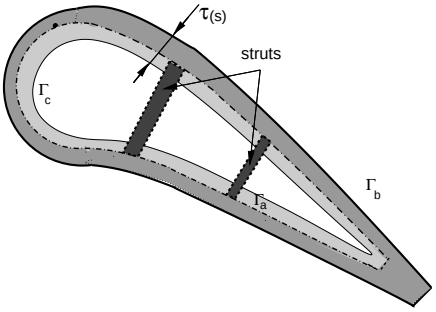

(a)

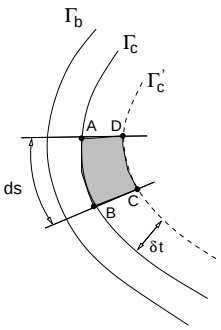

(b)

Figure 3: Domain geometry nomenclature (a) and domain area variation (b) for a hollow blade with a thickness based representation of coolant passages (Parametrization C).

written as

$$\Gamma_j \in R^2: \quad x = \sum_j \mu_j p_j(s), \qquad y = \sum_j \nu_j q_j(s) \quad (3)$$

where $p_j(s),\ q_j(s)$ are shape functions and μ_j, ν_j are the control parameters. The latter can be packed in a single vector α_i. In general, the optimal temperature field must satisfy the governing equation (1) and some geometric constraints. In order to solve such constrained extremum problem, we introduce the Lagrangian function

$$\mathcal{L}(T, \Gamma, \Lambda) = \mathcal{F}(\Gamma_c, T) + \int_\Omega \Lambda \, \nabla \cdot (\boldsymbol{k} \, \nabla T) d\Omega \quad (4)$$

where $\Lambda(\boldsymbol{x})$ is a Lagrange multiplier. The Lagrangian will allow us to treat the problem as unconstrained. A stationary configuration is found when the variation of $\mathcal{L}$ with respect to all its arguments, that are now considered independent functions, is 0. We compute $\delta\mathcal{L}$ as

$$\delta\mathcal{L} = \delta\mathcal{L}_T + \delta\mathcal{L}_\Lambda + \delta\mathcal{L}_{\Gamma_j} \quad (5)$$

All the contributions to $\delta\mathcal{L}$ must be 0 at the minimum. Hence, to find a stationary point we enforce

$$\delta\mathcal{L}_T = 0 \qquad \delta\mathcal{L}_\Lambda = 0$$

In general this results in $\delta\mathcal{L}_{\Gamma_j} \neq 0$. To reach the minimum we take $\delta\Gamma_j$ such that $\delta\mathcal{L} = \delta\mathcal{L}_{\Gamma_j} < 0$.

Note that the variations of $\mathcal{L}$ with respect to the Lagrange multipliers Λ simply yield the heat conduction equation. The condition $\delta\mathcal{L}_T = 0$ leads to the adjoint equation and its boundary conditions. Based on the second Green's identity the second integral can be formulated as

$$\begin{aligned}
\delta\mathcal{L}_T &= \int_\Omega \Lambda \, \nabla \cdot (k \nabla(\delta T)) d\Omega + \int_{\Gamma_b} (T - T_b)(\delta T) d\Gamma = \\
&= \int_\Omega (\delta T) \, \nabla \cdot (k \nabla \Lambda) d\Omega + \int_\Gamma \Lambda k \nabla(\delta T) \cdot \boldsymbol{n} \, d\Gamma \\
&- \int_\Gamma (\delta T) \, \boldsymbol{k} \, \nabla\Lambda \cdot \boldsymbol{n} \, d\Gamma + \int_{\Gamma_b} (T - T_b)(\delta T) d\Gamma = \\
&= \int_\Omega (\delta T) \, \nabla \cdot (k \nabla \Lambda) d\Omega + \\
&\int_{\Gamma_b} \left(\Lambda k \frac{\partial(\delta T)}{\partial n} - (\delta T) \, \boldsymbol{k} \, \frac{\partial \Lambda}{\partial n} + (T - T_b)(\delta T) \right) d\Gamma + \\
&\sum_i^M \int_{\Gamma_i} \left(\Lambda k \frac{\partial(\delta T)}{\partial n} - (\delta T) \, \boldsymbol{k} \, \frac{\partial \Lambda}{\partial n} \right) d\Gamma
\end{aligned} \quad (6)$$

By perturbing the boundary conditions (1b,1c) we can write

$$\begin{aligned}
k \frac{\partial(\delta T)}{\partial n} &= -h(\delta T) \qquad && on\ \Gamma = \Gamma_b \\
k \frac{\partial(\delta T)}{\partial n} &= h(\delta T) \qquad && on\ \Gamma = \Gamma_j
\end{aligned} \quad (7)$$

Substituting in (6) and considering all this integral contributions must vanish, we have

$$\begin{aligned}
\nabla \cdot (k \nabla \Lambda) &= 0 && on\ \Omega \\
k \frac{\partial \Lambda}{\partial n} &= h\Lambda + (T - T_b) && on\ \Gamma_b \\
k \frac{\partial \Lambda}{\partial n} &= -h\Lambda && on\ \Gamma_j
\end{aligned} \quad (8)$$

The adjoint problem (8) is formally identical to system (1). By changing $\Lambda \leftarrow T$ and with slight modifications to the set of boundary conditions, the numerical method used to solve the thermal problem can be applied to the adjoint problem.

To derive the variations $\delta\mathcal{L}_{\Gamma_j}$ we observe that, from eq. (3) they are formally equivalent to (and therefore replaced by) the variations of the Lagrangian function against the control parameters α_i

$$\delta\mathcal{L}_\alpha = \sum_i \frac{\partial}{\partial\alpha_i}\left[\int_\Omega \Lambda\nabla\cdot(k\nabla T)\,d\Omega + \chi\mathcal{P}\right]\delta\alpha_i \tag{9}$$

that can be resumed as

$$\delta\mathcal{L}_\alpha = \sum_i \mathcal{G}_i\delta\alpha_i \tag{10}$$

where

$$\mathcal{G}_i = \frac{\partial}{\partial\alpha_i}\left[\int_\Omega \Lambda\nabla\cdot(k\nabla T)\,d\Omega + \chi\mathcal{P}\right] \tag{11}$$

At the n-th iteration, if we update α_i with

$$(\delta\alpha_i)^n = -\rho\mathcal{G}_i^n \tag{12}$$

by taking $\rho > 0$, then $\delta\mathcal{L}_\alpha \leq 0$. By iterating such a procedure, the minimum is eventually reached. This method, namely the Steepest Descent Method (SDM), has a slow convergence. Better convergence rates can be obtained with the Conjugate Gradient Method (CGM) [21], in which the correction $\delta\alpha$ at the iteration n is given as

$$(\delta\alpha_i)^n = (\delta\alpha_i)^{n-1} + \beta^n\mathcal{G}_i^n \tag{13}$$

where β^n is defined by the modified Polak-Ribière formula

$$\beta^n = \max\left(\frac{\sum_i \mathcal{G}_i^n(\mathcal{G}_i^n - \mathcal{G}_i^{n-1})}{\sum_i \mathcal{G}_i^{n-1}\mathcal{G}_i^{n-1}},\ 0\right) \tag{14}$$

The final expression of the terms $\mathcal{G}_i(\Gamma_i, T, \Lambda)$ depends on the adopted parametrization of the cooling passages geometry.

3.1 Remarks on well-posedness and convergence

It is well known that an inverse problem can be ill-posed, e.g. if unrealistic target temperature $T_b(s)$ are imposed [1]. When the procedure diverges for any choice of α_i^0, the designer can observe, from the analysis of the optimization sequence, where the system fails to realize the prescribed temperature. Moreover, he can identify the thermal field that realizes the nearest agreement with the target distribution $T_b(s)$. As long as $T_b(x)$ is prescribed "a priori", ill-posedness issues can exist. These problems are eliminated if the inverse problem is included in a wider optimization process, where $T_b(s)$ itself becomes a control variable and therefore it is restricted to vary only on the subspace of allowable temperature distributions by the adjoint method [12, 13].

Gradient based methods could be attracted by local minima. The latter often appear in multidisciplinary optimizations, when control variables with opposite tendencies are treated. This behaviour can affect the convergence rate but it does not necessarily infer a failure in finding the global minimum. A restarting strategy of the CGM, with a variable selection of the parameter ρ often solves the problem. Another cure is based on non-deterministic approaches in the step selection e.g. genetic algorithms or simulated annealing).

If the solution is not unique, it may happen that the system is attracted to a solution, while the designer is interested in another one. This problem could arise in any automated design system. It has not been encountered in present work and, in general, it is removed by an appropriate choice of the boundary conditions [13].

3.2 Derivation of an optimal temperature distribution $T_b(s)$

Questions may arise on how the designer could select the blade temperature distribution $T_b(s)$. As mentioned above, the inverse problem can be included in a wider optimization process, where $T_b(s)$ itself becomes a control variable. This choice also eliminates ill-posedness issues by constraining $T_b(s)$ to vary only on the subspace of allowable temperature distributions by the adjoint method [12, 13]. Although the present work is focused on the solution of the inverse problem, a possible procedure is briefly outlined for sake of completeness. Let us introduce the optimization problem of finding the optimal shape and external blade temperature distribution T_b that minimizes a selected blade performance through the cost function $\mathcal{H}(\boldsymbol{U}, T, T_b, \Gamma)$. In general, the complete aero-thermal problem should be considered, since $\mathcal{H}$ is a function of the flow variables vector $\boldsymbol{U}$. To restrict our analysis to a pure thermal problem, as in [15], we try to minimize, for instance, the mean blade temperature $\overline{T_b}$. The role of the mean blade temperature on the turbine performance is investigated in [16]. The functional $\mathcal{H}$ is therefore

$$\mathcal{H}(T,\Gamma) = \overline{T_b} = \frac{\displaystyle\int_{\Gamma_b} T(\boldsymbol{x})d\Gamma}{\displaystyle\int_{\Gamma_b} d\Gamma} \tag{15}$$

Additional constraints on the maximum temperature or on the temperature gradient can be imposed by a suitable selection for parametrization of $T_b(s)$ (e.g. as in [12] has ben done for wall pressure distribution in an aerodynamic shape optimization problem), or by penalization. The original functional $\mathcal{F}$ in Eq. (2) is modified as

$$\mathcal{F}'(\Gamma_c, T, T_b) = \mathcal{F}(\Gamma_c, T) + \chi_1\mathcal{H}(\boldsymbol{U}, T, T_b, \Gamma) \tag{16}$$

where χ_1 is a weight parameter. An additional term is introduced in the lagrangian function $\mathcal{L}$, so that Eq. (4)

becomes

$$\mathcal{L}(T,\Gamma,T_b) = \mathcal{F}(T,\Gamma,T_b) + \int_{\Gamma_b} \xi(T(\boldsymbol{x}) - T_b(\boldsymbol{x}))d\Gamma \quad (17)$$

where $\xi(s)$ is a lagrangian multiplier. Then, in the footsteps of the procedure explained in the previous section, $\delta\mathcal{L}$ is computed as

$$\delta\mathcal{L} = \delta\mathcal{L}_T + \delta\mathcal{L}_\Lambda + \delta\mathcal{L}_{\Gamma_j} + \delta\mathcal{L}_{T_b} + \delta\mathcal{L}_\xi \quad (18)$$

Again, all the contributions to $\delta\mathcal{L}$ must vanish at the minimum

$$\delta\mathcal{L}_T = 0, \qquad \delta\mathcal{L}_\Lambda = 0, \qquad \delta\mathcal{L}_\xi = 0$$

and $\delta\mathcal{L}_{\Gamma_j} \neq 0$ and $\delta\mathcal{L}_{T_b} \neq 0$. To reach the minimum we take $\delta\Gamma_j$ and δT_b such that $\delta\mathcal{L}_{\Gamma_j} < 0$. and $\delta\mathcal{L}_{T_b} < 0$. Let us neglect the mathematical derivation of the new adjoint problem, which is out of the scope of the present exemplification. The optimization procedure can be started by using the results of the thermal analysis on an initial blade configuration. The computed temperature profile on the external blade surface $T_w(s)$ can be set as initial try for $T_b(s)$. Then, the solution of the adjoint procedure gives the $\delta\Gamma_j$ and δT_b in order to update both geometry and target temperature profile. The procedure iterates until convergence.

The idea of nesting the inverse procedure in a wider optimization process, which refines the target temperature profile $T_b(s)$, can also be implemented by using other optimization frameworks that are not necessarily based on adjoint methods.

4 DOMAIN PARAMETRIZATION

Scope of this section is to derive a formulation of $\mathcal{G}_i$ able to parametrize the geometric optimization variables α_j and to include the necessary set of constraints.

4.1 Parametrization A

We consider circular cooling passages. The parametric representation of the boundary $\Gamma_j(x,y)$ of each of M coolant passages is defined by

$$\begin{aligned} x(\vartheta) &= a_j + R_j\cos\vartheta \\ y(\vartheta) &= b_j + R_j\sin\vartheta \qquad\qquad 1 \le j \le M \end{aligned} \quad (19)$$

where $C_j = (a_j, b_j)$, R_j are the center and radius of the j-th circle, respectively (see Fig. 1). The vector of $3M$ control variables can be packed in a single vector as

$$\{\alpha\} = \{\{a_j\},\ \{b_j\},\ \{R_j\}\}, \qquad 1 \le j \le M \quad (20)$$

Letting a variation $\alpha_i \leftarrow \alpha_i + \delta\alpha_i$, and neglecting higher order terms, the functional $\mathcal{G}_i$ can be reduced to

$$\mathcal{G}_i = \begin{cases} \displaystyle\int_{\Gamma_i} \Lambda\nabla\cdot(k\nabla T)\frac{(x-\alpha_i)}{R_i}\,d\vartheta + \chi\frac{\partial\mathcal{P}}{\partial\alpha_i} \\ \qquad\qquad 1 \le i \le M \\ \displaystyle\int_{\Gamma_i} \Lambda\nabla\cdot(k\nabla T)\frac{(y-\alpha_i)}{R_{i-M}}\,d\vartheta + \chi\frac{\partial\mathcal{P}}{\partial\alpha_i} \\ \qquad\qquad M+1 \le i \le 2M \\ \displaystyle\int_{\Gamma_i} \Lambda\nabla\cdot(k\nabla T) r\,d\vartheta + \chi\frac{\partial\mathcal{P}}{\partial\alpha_i} \\ \qquad\qquad 2M+1 \le i \le 3M \end{cases} \quad (21)$$

Note that in eq. (20) the vector α_i is composed by three set of control variables (a_j, b_j, R_j), therefore we are now led to a formulation of $\mathcal{G}_i$ in which the three different contributions have been distinguished.

4.2 Parametrization B

As natural extension of the Parametrization A, the generic coolant passage can be represented by a polar distribution of radii $r(\theta)$ emanating from a given centroid C_j, as shown in Fig. 2a . Then, each contour can be approximated by a Fourier expansion

$$r(\vartheta) = A_1 + \sum_{n=1}^{M}\left[A_{(2n)}\sin(n\vartheta) + A_{(2n+1)}\cos(n\vartheta)\right] \quad (22)$$

where M is the number of harmonics. Each curve Γ_j can be expressed as

$$\mathbf{x}_j(\vartheta) = \mathbf{C}_j + r(\vartheta)(\cos(\vartheta)\,\hat{\mathbf{i}}_x + \sin(\vartheta)\,\hat{\mathbf{i}}_y) \quad (23)$$

being $\hat{\mathbf{i}}_x, \hat{\mathbf{i}}_y$ the unit vectors in the x and y-direction, respectively. If $0 \le \vartheta \le 2\pi$, then the whole passage is let vary during the inverse problem solution, and any additional geometric constraint can be introduced only by penalization. Partially fixed contours, e.g. to take into account for the presence of struts, can be introduced by excluding the angular extension of the region of interest from the optimization domain (i.e. $\vartheta_{min} \le \vartheta \le \vartheta_{max}$). Every time it is possible, the use of penalization should be avoided.

The integral function $\mathcal{G}$ can be evaluated as follows. Moving $\alpha \leftarrow \alpha + \delta\alpha$ implies $\Gamma_c \leftarrow \Gamma_c'$ (see Fig. 2b) and the variation $\delta\Omega$ can be approximated by

$$\delta\Omega \cong \delta\left(r(\vartheta)^2\frac{d\vartheta}{2}\right) \cong [r(\vartheta)d\vartheta]\delta r(\vartheta) \quad (24)$$

and therefore

$$\mathcal{G}_i = \int_{\Gamma_i} \Lambda\nabla\cdot(k\nabla T)\,r(\vartheta)\,d\vartheta + \chi\frac{\partial\mathcal{P}}{\partial\alpha_i} \quad (25)$$

4.3 Parametrization C

For hollow blades as in Fig. 3 , a more efficient description of the internal geometry is obtained by adding the thickness distribution to the external blade contour Γ_b (or to Γ_a). The thickness distribution $t(\eta)$ can be represented by any periodic interpolation function. For instance,

$$t(\eta) = A_1 + \sum_{n=1}^{M} \left[A_{(2n)} \sin(2\, n\pi\eta) + A_{(2n+1)} \cos(2n\pi\eta) \right] \tag{26}$$

the curve Γ_c is expressed as

$$\mathbf{x}_c(\eta) = \mathbf{x}_b(\eta) - t(\eta)\, \boldsymbol{n}_b(\eta) \tag{27}$$

being $\boldsymbol{n}_b(\eta)$ the normal vector to Γ_b along the normalized curvilinear coordinate η . One advantage is that this representation inhibits possible overlaps between coolant holes boundaries, so that the related terms of the penalization function can be dropped out. Moreover, Parametrization C still applies for partially fixed geometries of the coolant flow passage,e.g. when struts or surface coolant ejection channels are present. Finally, as shown in Fig. 3b, when $\Gamma_c \leftarrow \Gamma_c'$, by approximating the area variation $\delta\Omega$ by the quadrilateral ABCD, we are lead to

$$\delta\Omega \cong 2\, ds\, \delta\tau(s) \tag{28}$$

where second order terms have been neglected.

$$\mathcal{G}_i = 2 \int_{\Gamma_i} \Lambda \nabla \cdot (k \nabla T)\, ds + \chi \frac{\partial \mathcal{P}}{\partial \alpha_i} \tag{29}$$

4.4 Penalization

The holes boundaries cannot intersect each other and must lie far from the coating region of the blade. These requirements are constrains of the optimization problem and are introduced using penalization. When the coolant passages pattern is represented by a set of simple geometrical objects (e.g. circles, ellipses, ecc..) a strong penalization function is required to enforce non-intersecting conditions [5, 6, 14] . In parametrization B it is sometimes possible to avoid the use of penalization if the initial condition and the iterative update of the geometry is under-relaxed. Moreover, as long as centroids C_j are retained fixed during the optimization process, the non-intersecting condition can be guaranteed by limiting the domain of search by a frontier $(\Gamma_c)_{max}$. The same procedure can be used in parametrization C, where crossing boundaries Γ_j are less frequently observed in very elongated coolant flow passages, near the blade trailing edge. In the general case, the non-intersecting condition is enforced in a way similar to [5]. Considering M coolant passages, we write the penalization function as

$$\mathcal{P} = \sum_{i}^{M} \frac{d_0}{d_{ai} - d_0} + \sum_{j}^{M} \sum_{i=1, i\neq j}^{M} \frac{d_f}{d_{ij} - d_f} \tag{30}$$

where:

$d_{a\,i} = \min(||P_a - P_i||$

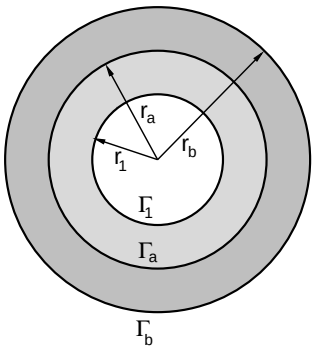

Test Case parameters	
Inner flow temperature [K]	$T_c = 603.15$
external flow temperature [K]	$T_g = 303.15$
inner core thermal conductivity $[W/mK]$	$k_1 = 15$
inner core thermal conductivity $[W/mK]$	$k_2 = 0.2$
inner walls heat transfer coefficient $[W/m^2K]$	$h_c = 400$
blade surface heat transfer coefficient $[W/m^2K]$	$h_g = 60$
outer cylinder radius [mm]	$r_b = 58$
inner cylinder radius [mm]	$r_1 = 25$
coating radius [mm]	$r_a = 38$

Figure 4: Composite hollow cylinder test-case.

is the minimum distance between the i-hole surface and the Γ_a contour (see Figs 1-3) and

$d_{ij} = \min ||(P_i - P_j)||$

is the minimum distance between two coolant passage contours Γ_i and Γ_j.

In [14] a detailed derivation of the penalization function for parametrization A is given. It must be noted that the penalization is often problem-dependent and the general way to deduce the gradient $\partial\mathcal{P}/\partial\alpha_i$ is by using automated differentiation tools.

5 NUMERICAL RESULTS

The proposed procedure is a classical optimization technique via adjoint equations. It consists of following steps:

1. solve the direct problem of equation (1).
2. solve the adjoint problem of equation (8).
3. evaluate the objective functional gradient by using equation (9).
4. compute the conjugate direction of search via equation (13) and march towards the extremum.
5. update the solution and test the convergence criterion.

The process starts with the selection of a suitable parametric representation α_i^0 of the blade internal geometry. Based on this initial set, the domain boundaries are deduced and

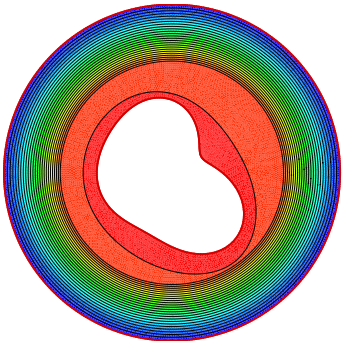

(a)

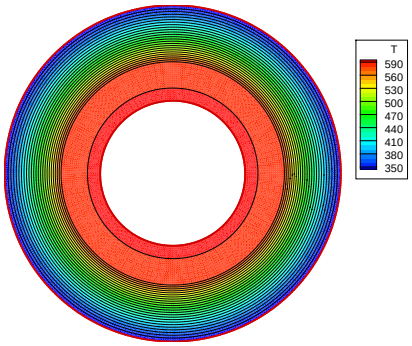

(b)

Figure 5: Composite hollow cylinder test-case. Initial (a) and final (b) domain geometry with the related temperature field.

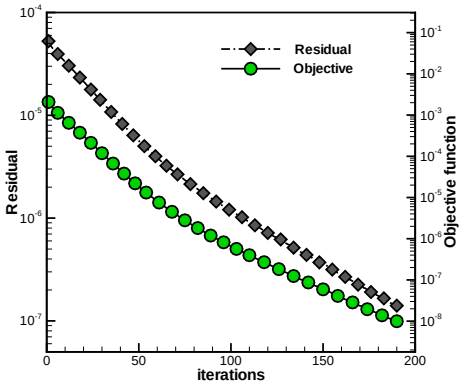

(a) Convergence history

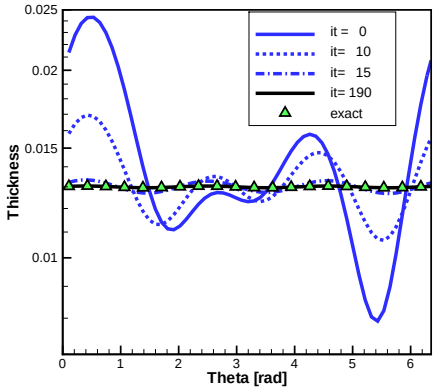

(b) Thickness distribution

Figure 6: Composite hollow cylinder test-case. (a) Objective function and L^2-norm of the controls residual versus iteration steps. (b) Cylinder thickness distribution $\tau(\vartheta)$ at selected iterations.

the mesh is generated. Then the FEM analysis (Step 1) is performed, using the best available information about the heat transfer coefficient h distributions along the blade surface and on the coolant channels. Although this solution has not be implemented here, conjugate heat transfer can be considered at this point and $h(\Gamma, s)$ can be extrapolated from an aero-thermal analysis. The adjoint problem (8) is solved on the same mesh and by the same FEM solver as in Step 1; the adjoint thermal field is used to compute the gradient of the objective function $\mathcal{F}(\Gamma_c, T)$. Finally, the CGM strategy identifies the search direction and the parametric representation is updated to the new set of control variables α_i^n . Step 1 is then applied to new internal blade configuration, and the L^2-norm residual of the control variables α_j, as well as the objective functional, are used to check the convergence level.

The whole numerical procedure has been implemented as a parallel FEM application as described in [14]. By using the meshing tool *bamg* [20], an adaptive mesh refinement with error control is performed to accurately resolve the thermal and the adjoint fields. As a consequence, at each iteration both thermal field and grid are computed twice. Although the resulting numerical procedure is not very efficient, it ensures a better grid resolution and a more accurate evaluation of the gradients. As far as 2D simulations are concerned, the computational remains quite affordable. Moreover, the computational cost of this adjoint procedure is independent to the number of control variables.

Three numerical applications are proposed in the next subsections. The first example is a test against an analytical solution. The second and third tests are based on experimental and numerical aerothermal analyses of cooled turbine blades [18, 19].

5.1 Coated cylinder with internal heating

Let us consider the heat transfer problem on a composite hollow cylinder with coating and a single circular heating passage as shown in Figure 4. The exact solution of the temperature field on the whole domain is obtained by classical analytical methods (e.g. [17], page 63, example 3-11). Although the test does not refer to a cooling problem it is proposed for comparison with previous works. In fact, this solution has been used to validate inverse procedures [5, 14]. Starting from a generic geometric configuration for the cylinder, as shown in Figure 5a, we solve for the geometry of the heating passage that realizes the target external wall temperature $T_w = T_b(\Gamma_b)$. The geometry of the inner passage is represented here using a Fourier series expansion eq. (22). The thermal field and the related adjoint problem are then solved at each optimization step

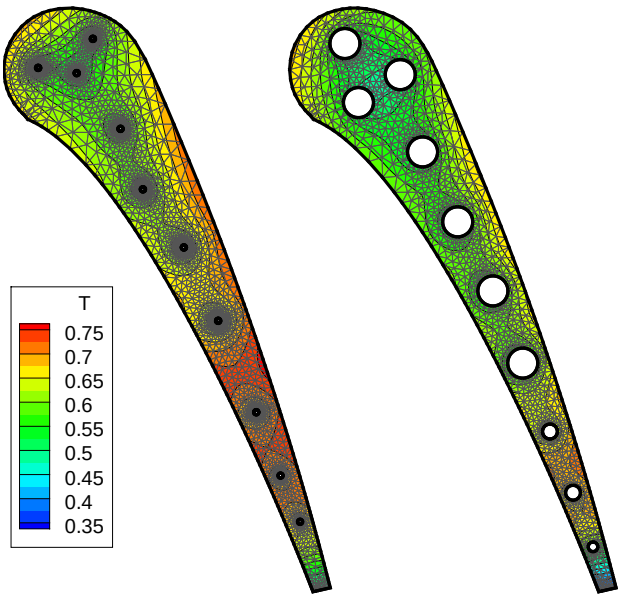

(a) (b)

Figure 7: Test Mark II. (a) Initial and (b) final grid and cooling passage pattern. the temperature field is normalized to $T_{ref} = 811$ K.

and the domain geometry is updated following eq. (13) by the CGM strategy and adaptive refinement, as discussed in the previous section. FEM domain discretization is based on quadratic triangular elements.

The generic initial condition and the final temperature field and geometry, characterized by a circular inner channel, are both shown in Figure 5 . The system has shown a monotonic convergence, as visible in Figure 6a where the function $\mathcal{F}$ and the L^2-norm residuals of α_i is plotted versus the optimization steps. The numerical results proposed are based on the parametrization C: a thickness distribution $\tau(\vartheta)$ is subtracted to the fixed coating frontier Γ_a to derive the internal channel geometry Γ_c. The penalization function $\mathcal{P}$ has been switched off. The evolution of the function $\tau(\vartheta)$ during the adjoint optimization process is shown in Figure 6b . The constant value $\tau = 0.013$ corresponds to the theoretical solution. If the center of circle Γ_b is chosen as the centroid, we have $r(\vartheta) = R_b - \tau(\vartheta)$. In this case the use of parametrization B or C leads to the same accuracy and convergence rates. A test using Parametrization A has been already presented in [14] and in that case penalization cannot be avoided, but also the control variables was only three: (x_1, y_1, R_1) .

5.2 Mark II turbine blade

Experimental data about the Mark II and CF3X internally cooled turbine blades are available in the open literature [18] and have been used as a reference test-case in several work on the conjugate heat transfer and optimal blade design. The Mark II stator vane geometry is depicted in

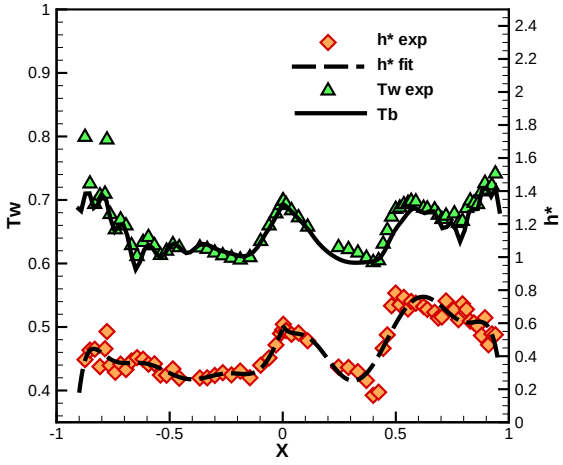

Figure 8: Test Mark II. Target temperature and heat transfer coefficient h^* on the blade surface. The normalization constants are: $T_{ref} = 811$ K and $h_{ref} = 1135\ W/(m^2K)$.

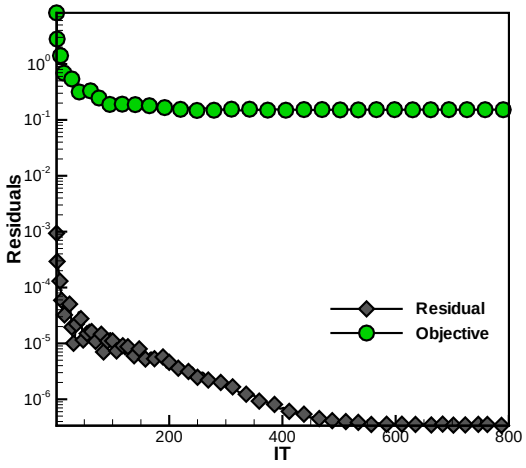

Figure 9: Test Mark II. Convergence history of the objective function and L^2-norm of the controls residual.

Figure 7b . The cooling system of this blade is composed by ten circular passages ($M = 10$). The experimental data are used here to formulate a design problem and to solve it by the inverse numerical procedure. The measured surface temperature for a selected working condition (namely, the *run-15* in[18]) is assumed as target temperature $T_b(\boldsymbol{x})$. Then, starting from an arbitrary initial geometry, the correct coolant passage pattern is sought. The control variables are the centre coordinates and radii of the circular cooling passages (parametrization A), packed in the vector α_i by (20) . The distribution of $h(s)$ along the external blade surface is based on a polynomial fitting of the experimental data. For the coolant passages, the heat transfer coefficient is obtained from the Nusselt number

$$Nu_D = C_r \cdot 0.022\, Pr^{0.5} {Re_D}^{0.8} \tag{31}$$

where Pr and Re are the Prandtl and Reynolds numbers based on the coolant flow rate, viscosity and temperature.

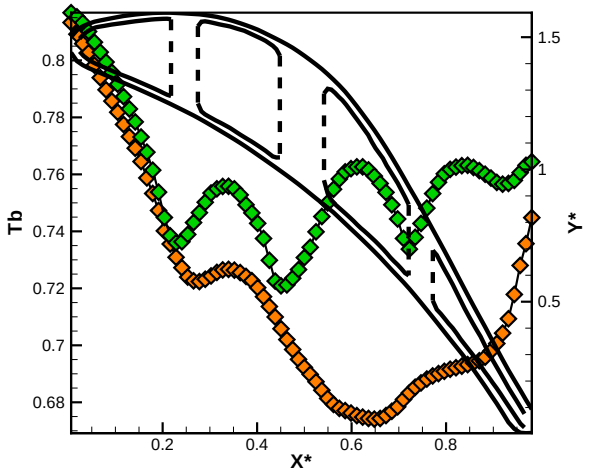

Figure 10: Hollow turbine blade. Blade geometry and target wall temperature profiles. Temperature is normalized to the reference $T_{ref} = 1651$ K.

C_r is an empirical correction parameter reported in [18] ($C_r = 1.118$ for hole 1 to 7, $C_r = 1.056$ for hole 8 and 9, $C_r = 1.025$ for hole 10).

The generic initial condition and the converged solution of the inverse procedure are shown in Figure 7. The test was quite severe: there are $3 \times M = 30$ control variables and, from eq. (30), $M \times M = 100$ penalty sub-functions to guarantee non-intersecting conditions on hole-to-hole and hole-to-external boundary. The experimental and the evaluated blade surface temperature are reported in Figure 8. The convergence of the objective functional and of the L^2-norm of the α_i residual are monitored in Figure 9. As visible, both functions decrease of two orders of magnitude in about 100 iterations. The geometrical configuration obtained is very close to the real one. For each α_i the relative error is less than 0.5% . By using the parallel implementation of the FEM code, the full computation (800 iterations) has run in about one hour on a 8-core Intel i7 workstation.

5.3 Hollow turbine blade

An aero-thermal analysis reported in [19] has been used as reference to test the inverse procedure on a configuration closer to modern hollow blades. Although the dataset in [19] does not disclose all information we need, it was the most complete we found in the open literature. The blade geometry and temperature profiles on the outer surface reported in [19] are shown in Figure 10. The blade is characterized has four coolant passages, while the presence of a coating barrier is not reported. The geometry was scaled by an unknown reference length, and also the heat transfer coefficient along the external blade surface was not given. Available data are the inlet total temperature ($T^0 = 1651$ K), the coolant fluid temperature ($T_c = 900$ K) and coolant wall average heat transfer coefficient ($h_c = 2000\ W/m^2\,K$), the blade thermal conductivity ($\kappa = 25\ W/m\,K$). Before proceeding further, we had to complete the dataset by introducing additional assumptions. In fact the knowledge of a reference solution (i.e. the geometry, the thermal field and heat fluxes) is required for testing the numerical procedure. First, the blade axial chord is arbitrarily set to $c_{ax} = 0.05$ m . The local heat flux q_w at a point $\boldsymbol{x}_p$ on the coolant passage walls is computed as suggested in [19] as

$$q_w(\boldsymbol{x}_p) = \frac{h_c\,(T_w(\boldsymbol{x}_p) - T_c)}{\kappa} \tag{32}$$

with the above-mentioned values for h_c, T_c and κ. This thermal boundary condition does apply also during the inverse procedure.

Then, a rough estimate of the heat transfer coefficient along the blade is deduced via the recovery temperature concept. Assuming a linear behaviour for both the Mach number $M_e(s)$ and for the static temperature $T_e(s)$ on the external flow along the blade, the recovery temperature is evaluated as

$$T_r(s) = T_e(s)\left(1 + r\,\frac{\gamma - 1}{\gamma} M_e^2(s)\right) \tag{33}$$

where, for a fully turbulent case, the recovery factor can be expressed as $r = (Pr)^{0.33}$, and the Prandtl number is $Pr = 0.72$ [17]. By imposing the known wall temperature distribution $T_b(s)$, the thermal field is computed by a FEM analysis. Finally, the heat transfer coefficient distribution is evaluated from the mixed boundary condition on the external blade surface

$$h_b(s) = \frac{k}{T_r(s) - T_b(s)} \left(\frac{\partial T}{\partial n}\right)_b \tag{34}$$

Now the reference solution is complete and we can build up a test-case exactly as done in the previous sections. Starting from the generic initial condition depicted in Figure 11a, the inverse procedure imposes the reference boundary conditions until the reference geometry is recovered with a satisfactory level of approximation. Using parametrization B, the procedure has failed to converge, since the centroid based representation has experienced problems in capturing the contour variation of very elongated coolant passages. By using the thickness based parametrization C, instead, the correct geometry has been found with a nearly monotonic convergence rate. The α_i residual is decreased of three order of magnitude, as visible in Fig. 12a . The snapshots of the thickness distribution at various iterations are plotted in Fig. 12a , where also target and obtained distributions are indistinguishable. Initial and final temperature field are shown in Figure 11. From numerical experiments, it was also observed that the use of penalization can be often avoided by starting with a very thin-walled blade and then let the procedure to increase slowly the wall thickness. In any case, parametrization C needs only the first term of eq. (11) to be implemented. The most critical channel to design is the one closest to the trailing edge. It is the first contour to overlap when thickness increases. Some numerical difficulties in the reconstruction of the channel contour can be also experienced in regions where the external boundary exhibits small radii

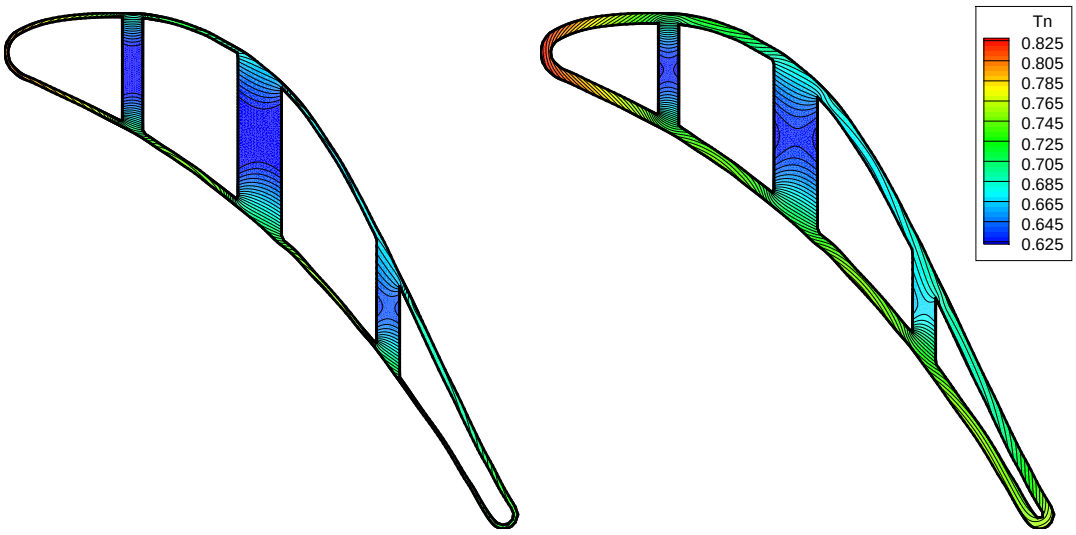

(a) (b)

Figure 11: Hollow turbine blade. (a) Initial and (b) final geometry and temperature field. Temperature is normalized to the reference $T_{ref} = 1651$ K.

of curvature. In this case a polynomial representation of curves is recommended in the leading and trailing edge zones, where the normal vector must be evaluated with high accuracy.

6 ACKNOWLEDGEMENTS

This work has been supported by the European Union under the FP7 project CRESCENDO (Collaborative and Robust Engineering using Simulation Capability Enabling Next Design Optimization).

7 CONCLUSIONS

An adjoint procedure for the solution of the inverse heat conduction problem, proposed in [14], has been reformulated with three different parametric representation of the internal cooling system of turbine blades. The algorithm can account for partially fixed geometry of internal passages, reducing or avoiding the need of penalization functions in the optimization problem. Moreover, if compared to similar approaches, the present adjoint formulation does not require the evaluation of an additional perturbation field. This reduces the computational cost and increases the robustness of the numerical technique. The computational cost is affordable on a medium level workstation. The procedure has been validated against analytical, experimental and numerical solutions. In all the test cases proposed, the method converges monotonically to the target solution. The bare-bone of the extension to the three-dimensional case is under testing as a web based application for concurrent design. In fact, the computational procedure can be implemented by using a scripting language and any command driven FEM solver that allows for the treatment of non-standard boundary conditions. In the future, the coupling with an aero-thermal analysis tool could be the natural extension of the method. Nevertheless, the open frontier is the robust design of turbine blades under specified thermal transients. As a starting point towards this direction, we remark that the adjoint equation can be also formally derived for the unsteady heat conduction equation.

References

[1] **Necati Özisik, M., Orlande, H. R. B.**, 2000, *Inverse Heat Transfer*, Taylor & Francis, London.

[2] **Alifanov, O.M.**, *Inverse Heat Transfer Problems*, Springer-Verlag, Berlin, 1994.

[3] **Beck, J.V., Blackwell, B., St. Clair, C.**, *Inverse heat conduction: Ill-posed problems*, Wiley, New York, 1985.

[4] **Kurpisz, K., Nowak, A. J.**, *Inverse Thermal Problems*, Computational Mechanics Publications, Southampton, UK and Boston, 1995.

[5] **Chiang, T. L., Dulikravich, G. S.**, 1986, "Inverse Design of Composite Turbine Blade Circular Coolant Flow Passages", *ASME Journal of Turbomachinery*, Vol. 108, pp. 275-282.

[6] **Dulikravich, G. S., Martin, T.J.**, 1994, "Inverse Design of Super-elliptic Cooling Passages in Coated Turbine Blades", *International Journal of Thermophysics and Heat Transfer*, Vol. 8(2), pp. 288–94.

[7] **Kennon, S. R., Dulikravich, G. S.**, "The Inverse Design of Internally Cooled Turbine Blades", 1985,

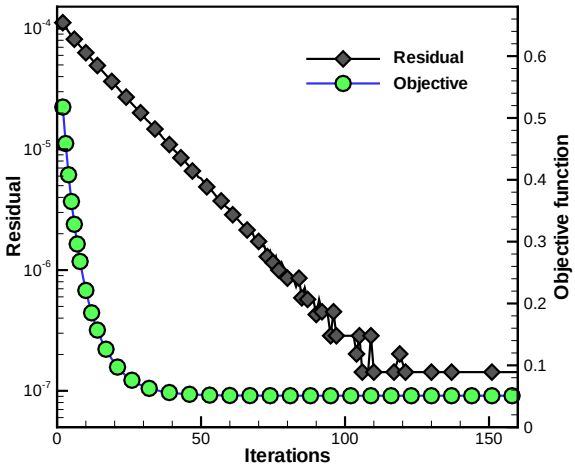

(a) Convergence history

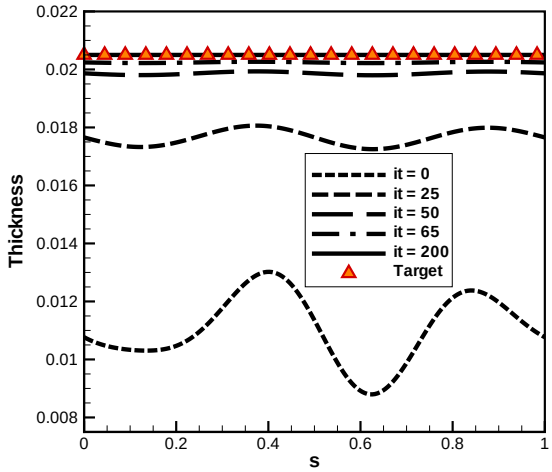

(b) Thickness profiles

Figure 12: Hollow turbine blade. (a) Objective function and L^2-norm of the controls residual versus iteration steps. (b) Blade thickness distribution $\tau(s)$ at selected iterations.

ASME Journal of Engineering for Gas Turbines and Power, Vol. 107, pp. 123-126.

[8] **Huang, C. H., Hsiung, T. Y.**, 1999, "An Inverse Design Problem of Estimating Optimal Shape of Cooling Passages in Turbine Blades", *International Journal of Heat and Mass Transfer*, Vol. 42, pp. 4307-4319.

[9] **Montomoli, F., Adami, P., Martelli, F.**, 2009, "A finite-volume method for the conjugate heat transfer in film cooling devices", *Journal of Power and Energy, Proceedings of the Institution of Mechanical Engineers, Part A*, Vol. 223, pp. 191-200.

[10] **Huang, C. H., Chen, C. W.**, 1998, "A boundary element based inverse-problem in estimating transient boundary conditions with conjugate gradient method", *International Journal of Numerical Methods in Engineering*, Vol. 42, pp. 943–658.

[11] **Huang, C. H., Wang, S. P.**, 1999, "A three-dimensional inverse heat conduction problem in estimating surface heat flux by conjugate gradient method", *International Journal of Heat and Mass Transfer*, vol. 42, pp. 33873403.

[12] **Iollo, A., Ferlauto, M., Zannetti, L.**, 2001, "An aerodynamic optimization method based on the inverse problem adjoint equations", *Journal of Computational Physics*, Vol. 173, pp. 87–115.

[13] **Ferlauto, M., Iollo, A., Zannetti, L.**, 2004, "Set of Boundary Conditions for Aerodynamic Design", *AIAA Journal*, Vol. 42, pp. 1582–92.

[14] **Ferlauto, M.**, 2013, "Inverse design of internally cooled turbine blades based on the heat adjoint equation", *Inverse Problems in Science and Engineering*, Vol. 2, pp. 269–282.

[15] **Talyaa, S.S., Chattopadhyaya A., Rajadasb, J.N.**, 2002, "Multidisciplinary Design Optimization Procedure for Improved Design of a Cooled Gas Turbine Blade", *Engineering Optimization*, Vol. 34, pp. 175–194.

[16] **Martin, B.W., Brown, A., Finnis, M.**, 1997, "The influences of turbine blade mean temperature and component efficiencies on coolant optimization in the gas turbine", *Proceedings of the Institution of Mechanical Engineers, Part A: Journal of Power and Energy*, Vol. 211, pp. 181–190.

[17] **Necati Özisik, M.**, 1985, *Heat Transfer, a basic approach*, McGraw-Hill, London.

[18] **Hylton, L. D., Millec, M. S., Turner, E. R., Nealy, D. A. , York, R. E.**, 1983, "Analytical and Experimental Evaluation of the Heat Transfer Distribution Over Surface of Turbine Vanes", *NASA-Report CR 168015*.

[19] **Han, Z., Dennis, B. H., Dulikravich, G. S.**,2 001, "Simultaneous prediction of External Flowfield and Temperature in Internally Cooled 3-D Turbine Blade Material", *International Journal of Turbo and Jet Engines*, Vol. 18, pp. 47–58.

[20] **Hecht, F., Kuate, R.**, 2008, "Metric Generation for a Given Error Estimation", *Proceedings of the 17th International Meshing Roundtable*, p.569–84, Garimella, Rao V. editors, Springer Verlag.

[21] **Fletcher, R.**, *Practical methods of Optimization*, John Wiley & Sons, 1980.